

# Effective Boundary Detection Using Color-Double Opponency And SSC

<sup>1</sup>Prof. Kalyankar P. P. , <sup>2</sup>Shivraj M. Nakate

<sup>1</sup>Department of Computer Engineering, <sup>2</sup>ME(CSE),

<sup>1</sup>TPCT's College Of Engineering, Osmanabad, India. <sup>2</sup>TPCT's College Of Engineering, Osmanabad, India.

## ABSTRACT

This system aiming two basic visual features, Brightness and color and to combine these two facts to maximize the reliability of boundary detection in natural scenes, we propose a new framework based on the color-opponent mechanisms of a certain type of color-sensitive double-opponent (DO) cells in the primary visual cortex of HVS(human visual system). Brightness and color are two basic visual features integrated by the human visual system (HVS) to gain a better understanding of color natural scenes. This type of DO cells has oriented receptive field with both chromatically and spatially opponent structure. The proposed framework is a feedforward hierarchical model, which has direct counterpart to the color-opponent mechanisms involved in from the retina to V1. In addition, we employ the spatial sparseness constraint (SSC) of neural responses to further suppress the unwanted edges of texture elements. Experimental results show that the DO cells we modeled can flexibly capture both the structured chromatic and achromatic boundaries of salient objects in complex scenes when the cone inputs to DO cells are unbalanced. Meanwhile, the SSC operator further improves the performance by suppressing redundant texture edges. With competitive contour detection accuracy, the proposed model has the additional advantage of quite simple implementation with low computational cost.

**Keywords:** Boundary, Color Opponent, Receptive Field, Visual System, Texture Suppression.

## I. Introduction

### 1.1 Boundary Detection

Boundary detection characterize object boundaries and are useful features for segmentation, registration and object identification in scenes. Goal of boundary detection is Identify sudden changes or discontinuities in an image. Boundaries of object represent important role for visual perception such as scene understanding and object recognition [1]. Boundary detection is also a fundamental building block for a large variety of computer vision applications, such as image segmentation and object detection[2],[3]. However, most traditional edge detection methods usually extract edges by computing the abrupt change of local luminance.

As a basic feature of external world, color information plays an important role in human visual perception such as shape and object recognition[6].

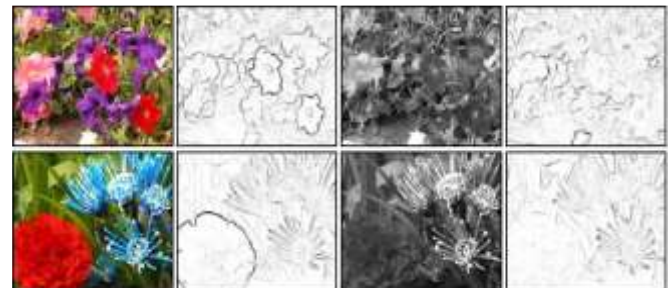


**Fig.1.1** Examples showing that color boundaries are lost when ignoring color information. Color images and their boundary maps (the first and second column) provide more object information than gray-level images and their boundary maps (the third and last column).

From the perspective of engineering, color is also necessary for various image processing tasks, such as edge detection[5],[7], image segmentation, junction/corner detection[8]. Fig. 1 shows typical examples illustrating that some important contours of objects (e.g., flowers in the first column) in color images are lost in the gray-scale space, especially for those boundaries with only color contrast in regions of iso-luminance.

## II. Related Work

### 2.1 Traditional Boundary Detection System

In order to detect boundaries from color images, many early studies focused on extending the standard edge detectors, such as Canny[4], to color space. These methods are inherently difficult to discriminate salient object boundaries and texture edges due that they respond to all the discontinuities in image intensity, color or texture. In recent decades, many new approaches have been developed for boundary detection in complex scenes. Typically, in the famous *Pb* method, Martin *et al*[5]. took into account multiple local cues (i.e., color, brightness, and texture) and combined these cues with certain learning technique to detect and localize the boundaries. Other learning-based methods tried to take multiple scales[9], more local features [10]or global information[2],[8] for better results. However, the performances of most learning-based methods mentioned above are dependent on the appropriate selection of training sets, which makes the methods inflexible for individual images. Furthermore, the high computational cost resulted from training needs to be carefully dealt with.

Another important issue is to make the salient contours pop out in cluttered scenes. There are mainly two classes of methods including contour grouping and texture suppression. Contour grouping methods usually integrate low-level elements produced by basic edge detectors into mid-level features. For example, Zhu *et al.* [12]proposed a contour grouping method with the topological formulation called Untangling Cycles.

Ren *et al* [13]. presented a model to enforce the curvilinear continuity with Conditional Random Fields framework. By utilizing the Gestalt rules (i.e., good-continuation, proximity, contour-closure, etc.), existing methods introduced the local interactions between contour segments [14],[15] and global effect [16] to extract perceptually salient contours. Salient contours were also extracted by solving the min-cover problem [17] or building Ultrametric Contour Maps [2],[18]. Texture analysis methods have also been used to suppress the undesired textured edges while extracting boundaries. These detectors respond well to texture-defined boundaries and are insensitive to unwanted edge segments within homogeneous textured regions. However, texon-based methods usually take high computational cost on multiple convolution operations and high-dimensional analysis. Recently, some more time-saving texture boundary detection algorithms have been proposed. For example, biologically inspired surround inhibition methods make texture boundaries pop out by suppressing the unwanted short edges surrounded by similar textured patterns [21],[22]. Hidayat *et al.* detected texture boundaries almost in real-time by extracting ridges in the standard deviation space [23].

#### 2.1.2 Color Mechanisms in Early Visual System

Color processing in the human visual system (HVS) progresses through a series of hierarchical steps [19],[26],[27]: after the light absorption by cone photoreceptors, cone activities are transmitted via horizontal cells, bipolar cells, etc, and then compared by cone-opponent retinal ganglion cells (RGCs); these color signals are transmitted via the Lateral Geniculate Nucleus (LGN) to the primary visual cortex (V1) and then higher cortical areas. One of the amazing properties in the early stages of HVS, i.e., retina  $\rightarrow$  LGN  $\rightarrow$  V1, is on the color coding, which can be summarized as follows:

- **Trichromacy:** The first stage of color processing of HVS takes place in the photoreceptor layer of the retina. There are two types of photoreceptors: rods and cones, and cones are responsible for color vision. There exist three kinds of cone photoreceptors, namely L, M, and S cones,

which preferably absorb long, middle, and short wavelengths in a local spatial space, respectively. This is well known as trichromacy. As described in many other literatures, in the following the L-, M- and S-cones will be also referred to as red (R), green (G), and blue (B) cones, though each cone class does not specifically code the perception of a single color of R, G or B. • Color opponency. Many researchers have reported that color information is processed in the visual pathway in an opponent way, i.e., red versus green (red-green, or R-G) and blue versus yellow (blue-yellow, or B-Y) channels. Responses to the two colors of an opponent channel are antagonistic to each other, which makes opposite opponent colors never be perceived together. For example, there is no color like “greenish red” or “yellowish blue”.

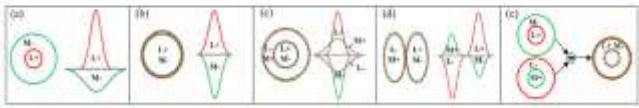


Fig.2.1 Color opponent cells

The receptive fields of single-opponent cells of Type I (a) and Type II (b) in RGC and LGN levels, and double-opponent cells in V1 with concentric RF(c) and oriented double-opponent cells in V1 with side-by-side spatially antagonistic regions with unbalanced cone weights (d). In the expression of “A+” or “B-”, the sign “+” and “-” denote the role of excitation and inhibition, respectively. Adapted from [19] and [20]. (e) An illustration to explain that the center-only RF of Type II in LGN is constructed by differencing two center-surround ganglion cells.

• **Color opponent cells:** The RGCs or LGN cells have been found to have single-opponent (SO) receptive field (RF) and some kinds of cells in V1 have double-opponent (DO) RF [19],[27]. There are mainly two types of singleopponent cells: Type I cells have center-surround opponent RF, and in contrast, Type II cells have center-only opponent RF. It has been found that these single-opponent cells come in four varieties, i.e., L-on/M-off (or L+M-), M-on/L-off (or M+L-), S-on/(L+M)-off (or

S+(L+M)-), and (L+M)-on/S-off (or (L+M)+S-), where “on” and “off” correspond to the RF center and surround, respectively. In V1, the RF of DO neurons shows more complex properties. Their RFs are both chromatically and spatially opponent [28], which was considered as an important role in color scene understanding [25]. Especially, it has been reported that some DO neurons in V1 have concentric centersurround RF or side-by-side spatially oriented RFs. The DO cells with concentric RF were thought to be physiological building blocks of color constancy and color contrast, and our previous model has shown that such DO cells contribute to color constancy by coding the external light source color [29],[30]. Differently, the DO cells with oriented RF, which will be specifically modeled in this study, have been assumed to play crucial role in boundary detection in (color) natural scenes[31]. Physiological experiments indicated that the DO cells can respond well to color-defined boundaries when the cone weights are well balanced [20], and can respond sensitively to both achromatic and isoluminant gratings when the cone weights are unbalanced [19],[27].

### III. Existing System

#### 3.1 Early System

- Among numerous computational boundary detection, typical methods include:

##### ➤ Canny detector :

This is probably the most widely used edge detector in computer vision Theoretical model: step-edges corrupted by additive Gaussian noise Canny has shown that the first derivative of the Gaussian closely approximates the operator that optimizes the product of signal-to-noise ratio and localization

Note about Matlab’s Canny detector

Small errors in implementation:



Gaussian function not properly normalized

First filters with a Gaussian, then a difference of Gaussian (equivalent to filtering with a larger Gaussian and taking difference).

- Zero crossing
- phase congruency

- In these above methods, to detect boundaries from color images, many early studies focused on extending the standard edge detectors, such as Canny to color space.
- However, most traditional edge detection methods usually extract edges by computing the abrupt change of local luminance.
- The performances of most learning-based methods mentioned above are dependent on the appropriate selection of training sets.

### 3.2 Limitations Of The Existing System

The existing or traditional Boundary detection system has some limitations which can be overcome by adopting new methods.

- These methods are inherently difficult to discriminate salient object boundaries and texture edges due that they respond to all the discontinuities in image intensity, color or texture.
- Normally are not capable of distinguishing boundaries from abundant of textured edges.

## IV. Proposed System

### 4.1 Proposed Work

This new boundary detection system is based on the double-opponent (DO) mechanism and has the amazing property of jointly extracting color- and luminance-defined edges, which is really different from the two-step way of some existing models that explicitly extract the color and luminance edges in separate channels and then combine them.

A new strategy of spatial sparseness constraint (SSC) was introduced to weight the edge responses of the proposed CO system, which provides a simple while efficient way for texture suppression.

This system proposes a novel contour detection model based on the color-opponent mechanisms of the biological visual system by specifically simulating the DO cells with oriented RF. The new model includes three layers simulating the levels of retina, LGN, and V1 (Fig. 3). Particularly, in the last layer (Cortex layer), a pool of oriented DO cells with different preferred orientations is used at each location to extract boundaries by receiving the responses of SO LGN cells, followed by a max operator across all orientations to combine responses to boundaries in separate DO channels. Finally, we compute the maximum to combine the boundaries across all DO channels. To our knowledge, this work is the first attempt to introduce the DO mechanism of color-sensitive V1 cells with oriented RF, a very important group of cells in V1, for detecting boundaries.

Second, this work also develops a new texture suppression method with spatial sparseness constraint (SSC). We suppress the neuronal responses to the edges in the local regions with low sparseness measure. This operator works well because the local regions containing (unwanted) regularly distributed textures tend to exhibit lower local sparseness measure, while the regions covering salient boundaries usually have high spatial sparseness in response.

As briefly mentioned above, in this work, we simulate the biological mechanisms of color information processing along the Retina-LGN-Cortex visual pathway and propose a feedforward hierarchical system for boundary detection in real natural scenes by using only low-level local information. The results on a commonly used dataset will show that our model has the capacity of jointly detecting the color- and luminance-defined boundaries and efficiently suppressing textural edges.

### 4.2.1 From Single- to Double-Opponent Processing

Our framework shown in Fig. 3 is a feedforward hierarchical model including three layers, which correspond to the levels of retina, LGN, and V1 of the visual system, respectively. Based on the physiological hypothesis that the two subregions of the RF of oriented DO cells resemble the RF of a Type II cell, we model that each DO V1 cell receives the

neuronal responses of two singleopponent LGN cells of Type II. In Fig. 3, we just show the computational steps in the R-G channel, and information processing along another channel of B-Y shares the similar computational steps.

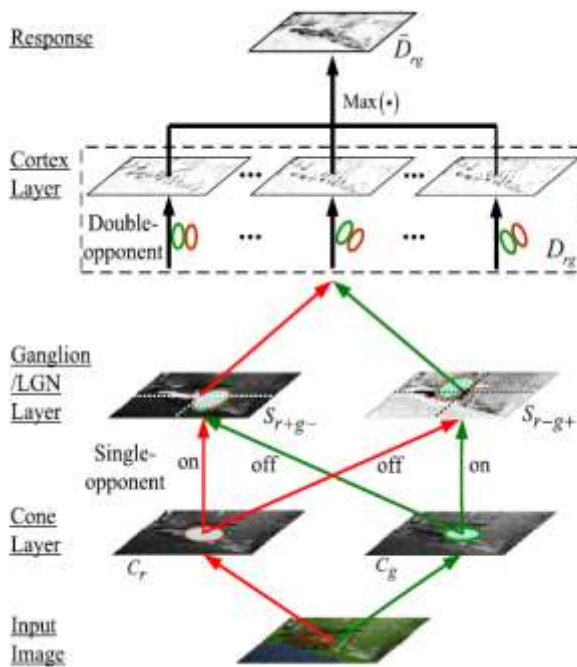


Fig.4.1 System Framework

1) **Cone Layer:** At the layer of cone photoreceptors, the input color image is first separated into three components:  $I_r(x, y)$  for red (R),  $I_g(x, y)$  for green (G), and  $I_b(x, y)$  for blue (B), which are respectively sent into L, M, and S cones. In addition, when the information from the cones is passed forward via horizontal cells, bipolar cells, etc., to the retinal ganglion cells, the output layer of the retina, a yellow (Y) component is constructed by a kind of bipolar cells that receive both R and G cone signals, i.e.,  $I_y(x, y) = 0.5(I_r(x, y) + I_g(x, y))$ , which will be then sent to the single-opponent ganglion cells of B-Y type.

## 2) Ganglion/LGN Layer:

The majority of ganglion cells in retina have center-surround RFs, which send information to LGN, a place that is widely regarded as a relay center between the retina and V1. Many physiological findings reveal that the ganglion

and LGN cells have similar RF properties (e.g., single-opponent), and the main difference is that LGN cells have relatively larger RFs. Meanwhile, physiological studies have also reported that Type II cells with center-only RFs do exist in the dorsal layers of LGN, though they are in the minority. It has been suggested that the RF of a Type II LGN cell could be constructed by differencing two center-surround SO ganglion cells. Based on this idea, we unify the ganglion and LGN layers into a single processing by center-only LGN cells.

## 3) Cortex Layer:

In the cortex layer of V1, the RFs of most color- and color-luminance-sensitive neurons are both chromatically and spatially opponent. Mathematically, the DO RF with two side-by-side spatially antagonistic regions can be modeled using the first-order (partial) derivative of a two-dimensional (2D) Gaussian.

### 4.2.2 Spatial Sparseness Constraint for Texture Suppression

Here we propose a new method to suppress the responses to unwanted textures by introducing the spatial sparseness constraint (SSC). It has been well recognized that our visual system represents the natural scenes with a quite efficient style, such as sparse coding [32], [33]. Sparse coding models have been used to account for the responsive properties of V1 neurons [33], [34]. From the perspective of engineering, sparse features have been trained to discriminate contours of objects [11]. In specific, Alpert *et al.* [35] employed the sparseness measure proposed in [36] to distinguish the textured and non-textured regions based on the assumption that the non-textured regions are fairly sparse. In order to narrow the unexpected spreading of high sparseness measure around the true boundaries, here we improve the computation of sparseness by introducing spatial information. Similar as Alpert *et al.*[35], we assume that the textured regions are far from sparse, with a low probability of containing wanted boundaries, considering the observation that the textured regions are often characterized by strong responses to edges at various orientations and scales [24]. Our strategy is as follows.

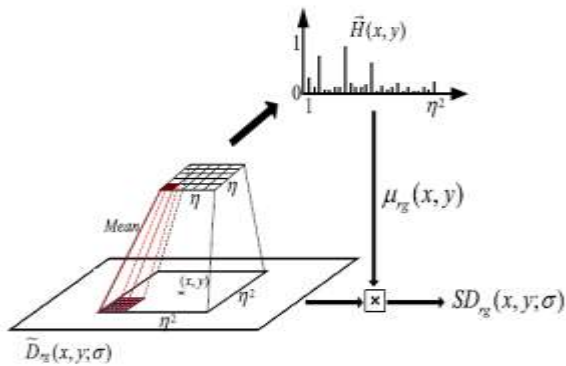


Fig. 4.2. The computation of texture suppression with SSC

For each location  $(x, y)$  of the boundary response, we compute the spatial sparseness measure of boundary response based on the information within a local window centered at  $(x, y)$ . Fig. 5 illustrates the steps of sparseness computation. In this work, we define a square window with a size of  $\eta^2 \times \eta^2$  pixels for the computation of spatial sparseness at each location. This window is further combined into  $\eta \times \eta$  sub-patches with the size of  $\eta \times \eta$  pixels, and the mean response magnitude is obtained for each sub-patch. Finally, the totally  $\eta^2$  mean magnitude values are arranged into a one-dimensional vector denoted by  $\_H(x, y)$ . Then,  $\mu_g(x, y)$ , the new sparseness measure of location  $(x, y)$ , is obtained by

$\mu_g(x, y) = \lambda(x, y) \cdot \text{sparseness}(x, y; \_H)$   
 $\lambda(x, y) = \min(1, \text{Drg}(x, y; \sigma) / \text{mean}\{ \_H(x, y) \})$   
 where  $\text{mean}\{ \_H(x, y) \}$  denotes the mean value of the elements of  $\_H(x, y)$ , which is equivalent to the mean response within the local window. Hence,  $\lambda(x, y)$  is a factor that acts to weight the sparseness measure of certain location based on the distribution of neuronal responses within its local region. The operator  $\min(\cdot)$  makes  $\lambda(x, y) \leq 1$ , indicating that  $\lambda(x, y)$  acts only to reduce the sparseness measure if necessary.

### 4.3 Basic Properties of the Proposed Approach

To begin with, we evaluate the effect of the

cone weights shown as  $w$  in Fig. 7 on the performance of the proposed model.

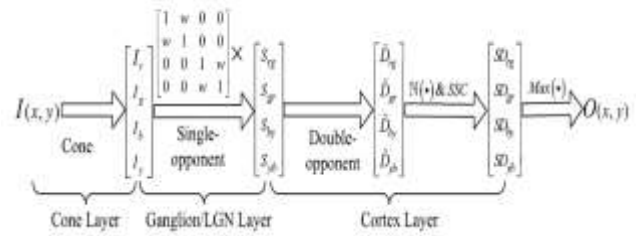


Fig. 4.3 The full steps of the proposed system

## V. Experiment Result

Results of this experiment is shown in following figure. We also evaluated the influence of SSC. Figs. 6 to 10 shows that the overall performance is improved when modified sparseness measure is used in SSC. That is, our both versions of modified SSC outperform the original sparseness measure, which has negligible contribution to performance.



Fig. Original Image



Single opponency Output



Entropy:0.50193  
 MSE:5344.6593    5467.7842    5054.07  
 PSNR:10.8516    10.7527    11.0944

Fig.9.image with single Opponency and their boundary maps.

Double opponency Output



Entropy:7.0777  
 MSE:0.79595  
 PSNR:10.8516    10.7527    11.0944

Fig.10. Final image with Double Opponency and their boundary maps.

### 5.1 Advantages Of Proposed System

- Competitive performance for edge detection and texture suppression with only low-level local information.
- Flexibility in responding to color- and luminance-defined boundaries.
- As few as only one free parameter (i.e., cone weight) (the model is almost insensitive to another parameter, Gaussian scale  $\sigma$ ).
- Quite low computational cost.
- A new strategy of spatial sparseness constraint (SSC) was introduced to weight the edge responses of the proposed CO

system, which provides a simple while efficient way for texture suppression.

## VI. Conclusion

This mechanism proposed a novel way for the challenging task of detecting salient boundaries in complex color scenes, inspired by the information processing mechanisms emerging in the early visual stages. In specific, the SO ganglion cells function to enhance region information, and the oriented DO cells in V1 serve to detect the boundaries among regions.

The main novelty of the work is summarized as follows. (a) Our new boundary detection system is based on the double-opponent (DO) mechanism and has the amazing property of jointly extracting color- and luminance-defined edges, which is really different from the two-step way of some existing models that explicitly extract the color and luminance edges in separate channels and then combine them, e.g., with a supervised learning. (b) A new strategy of spatial sparseness constraint (SSC) was introduced to weight the edge responses of the proposed CO system, which provides a simple while efficient way for texture suppression. The main merits of the proposed *SCO* model include: (a) competitive performance for edge detection and texture suppression with only low-level local information; (b) flexibility in responding to color- and luminance-defined boundaries; (c) as few as only one free parameter (i.e., cone weight  $w$ ) (the model is almost insensitive to another parameter, Gaussian scale  $\sigma$ ); (d) quite low computational cost.

## VII. References

- [1] D. B. Walther, B. Chai, E. Caddigan, D. M. Beck, and L. Fei-Fei, "Simple line drawings suffice for functional MRI decoding of natural scene categories," *Proc. Nat. Acad. Sci.*, vol. 108, no. 23, pp. 9661–9666, 2011.
- [2] P. Arbeláez, M. Maire, C. Fowlkes, and J. Malik, "Contour detection and hierarchical image segmentation," *IEEE Trans. Pattern Anal. Mach. Intell.*, vol. 33, no. 5, pp. 898–916, May 2011.
- [3] G. Papari and N. Petkov, "Edge and line oriented contour detection: State of the art," *Image Vis. Comput.*, vol. 29, nos. 2–3, pp. 79–103, 2011.
- [4] J. Canny, "A computational approach to edge detection," *IEEE Trans Pattern Anal. Mach. Intell.*, vol. PAMI-8, no. 6, pp. 679–698, Nov. 1986.

- [5] D. R. Martin, C. C. Fowlkes, and J. Malik, "Learning to detect natural image boundaries using local brightness, color, and texture cues," *IEEE Trans. Pattern Anal. Mach. Intell.*, vol. 26, no. 5, pp. 530–549, May 2004.
- [6] S. K. Shevell and F. A. Kingdom, "Color in complex scenes," *Annu. Rev. Psychol.*, vol. 59, pp. 143–166, Jan. 2008.
- [7] M. A. Ruzon and C. Tomasi, "Edge, junction, and corner detection using color distributions," *IEEE Trans. Pattern Anal. Mach. Intell.*, vol. 23, no. 11, pp. 1281–1295, Nov. 2001.
- [8] M. Maire, P. Arbeláez, C. Fowlkes, and J. Malik, "Using contours to detect and localize junctions in natural images," in *Proc. IEEE CVPR*, Jun. 2008, pp. 1–8.
- [9] X. Ren, "Multi-scale improves boundary detection in natural images," in *Proc. ECCV*, 2008, pp. 533–545.
- [10] P. Dollar, Z. Tu, and S. Belongie, "Supervised learning of edges and object boundaries," in *Proc. IEEE CVPR*, vol. 2, Jun. 2006, pp. 1964–1971.
- [11] X. Ren and L. Bo, "Discriminatively trained sparse code gradients for contour detection," in *Proc. NIPS*, 2012, pp. 593–601.
- [12] Q. Zhu, G. Song, and J. Shi, "Untangling cycles for contour grouping," in *Proc. IEEE 11th ICCV*, Oct. 2007, pp. 1–8.
- [13] X. Ren, C. C. Fowlkes, and J. Malik, "Scale-invariant contour completion using conditional random fields," in *Proc. 10th IEEE ICCV*, vol. 2, Oct. 2005, pp. 1214–1221.
- [14] R. Kennedy, J. Gallier, and J. Shi, "Contour cut: Identifying salient contours in images by solving a Hermitian eigenvalue problem," in *Proc. IEEE CVPR*, Jun. 2011, pp. 2065–2072.
- [15] S. Mahamud, L. R. Williams, K. K. Thornber, and K. Xu, "Segmentation of multiple salient closed contours from real images," *IEEE Trans Pattern Anal. Mach. Intell.*, vol. 25, no. 4, pp. 433–444, Apr. 2003.
- [16] Y. Ming, H. Li, and X. He, "Connected contours: A new contour completion model that respects the closure effect," in *Proc. IEEE CVPR*, Jun. 2012, pp. 829–836.
- [17] P. Felzenszwalb and D. McAllester, "A min-cover approach for finding salient curves," in *Proc. Comput. Vis. Pattern Recognit. Workshop (CVPRW)*, Jun. 2006, p. 185.
- [18] P. Arbelaez, "Boundary extraction in natural images using ultrametric contour maps," in *Proc. Comput. Vis. Pattern Recognit. Workshop (CVPRW)*, Jun. 2006, p. 182.
- [19] B. R. Conway *et al.*, "Advances in color science: From retina to behavior," *J. Neurosci.*, vol. 30, no. 45, pp. 14955–14963, 2010.
- [20] S. G. Solomon and P. Lennie, "The machinery of colour vision," *Nature Rev. Neurosci.*, vol. 8, no. 4, pp. 276–286, 2007.
- [21] C. Grigorescu, N. Petkov, and M. A. Westenberg, "Contour detection based on nonclassical receptive field inhibition," *IEEE Trans. Image Process.*, vol. 12, no. 7, pp. 729–739, Jul. 2003.
- [22] K.-F. Yang, C.-Y. Li, and Y.-J. Li, "Multifeature-based surround inhibition improves contour detection in natural images," *IEEE Trans. Image Process.*, vol. 23, no. 12, pp. 5020–5032, Dec. 2014.
- [23] R. Hidayat and R. D. Green, "Real-time texture boundary detection from ridges in the standard deviation space," in *Proc. BMVC*, 2009, pp. 1–10.
- [24] J. Malik and P. Perona, "Preattentive texture discrimination with early vision mechanisms," *J. Opt. Soc. Amer. A*, vol. 7, no. 5, pp. 923–932, 1990.
- [25] J. Zhang, Y. Barhomi, and T. Serre, "A new biologically inspired color image descriptor," in *Proc. ECCV*, 2012, pp. 312–324.
- [26] K. R. Gegenfurtner, "Cortical mechanisms of colour vision," *Nature Rev. Neurosci.*, vol. 4, no. 7, pp. 563–572, 2003.
- [27] R. Shapley and M. J. Hawken, "Color in the cortex: Single- and double-opponent cells," *Vis. Res.*, vol. 51, no. 7, pp. 701–717, 2011.
- [28] E. N. Johnson, M. J. Hawken, and R. Shapley, "The orientation selectivity of color-responsive neurons in macaque V1," *J. Neurosci.*, vol. 28, no. 32, pp. 8096–8106, 2008.
- [29] S. Gao, K. Yang, C. Li, and Y. Li, "A color constancy model with double-opponency mechanisms," in *Proc. IEEE ICCV*, Dec. 2013, pp. 929–936.
- [30] S. Gao, K. Yang, C. Li, and Y. Li, "Color constancy using doubleopponency," *IEEE Trans. Pattern Anal. Mach. Intell.*, Jan. 2015.
- [31] E. N. Johnson, M. J. Hawken, and R. Shapley, "The spatial transformation of color in the primary visual cortex of the macaque monkey," *Nature Neurosci.*, vol. 4, no. 4, pp. 409–416, 2001.
- [32] B. A. Olshausen and D. J. Field, "Emergence of simple-cell receptive field properties by learning a sparse code for natural images," *Nature*, vol. 381, no. 6583, pp. 607–609, 1996.



[33] M. Zhu and C. J. Rozell, “Visual nonclassical receptive field effects emerge from sparse coding in a dynamical system,” *PLoS Comput. Biol.*, vol. 9, no. 8, p. e1003191, 2013.

[34] M. W. Spratling, “Image segmentation using a sparse coding model of cortical area V1,” *IEEE Trans. Image Process.*, vol. 22, no. 4, pp. 1631–1643, Apr. 2013.

[35] S. Alpert, M. Galun, A. Brandt, and R. Basri, “Image segmentation by probabilistic bottom-up aggregation and cue integration,” *IEEE Trans. Pattern Anal. Mach. Intell.*, vol. 34, no. 2, pp. 315–327, Feb. 2012.

[36] P. O. Hoyer, “Non-negative matrix factorization with sparseness constraints,” *J. Mach. Learn. Res.*, vol. 5, pp. 1457–1469, Dec. 2004.

